SCIENTIFIC PAPER
Published: December 23, 2022
https://doi.org/10.13167/2022.25.4

Numerical Analysis of Geometric and Material Nonlinearity of Beams in the Plane

Besim Demirović[1], Nedim Osmić[2], Rašid Hadžović[3] and Zijad Požegić[4]

[1] *University of Tuzla, Faculty of Mining Geology and Civil Engineering, Department of Civil Engineering, Univerzitetska, 2, 75000, Tuzla, Bosnia and Herzegovina*

[2] *University of Tuzla, Faculty of Mining Geology and Civil Engineering, Department of Civil Engineering, Univerzitetska, 2, 75000, Tuzla, Bosnia and Herzegovina*

[3] *University of "Džemal Bijedić" in Mostar, Faculty of Civil Engineering, Department for Structures, Midhat Hujdur Hujka, 88104, Mostar, Bosnia and Herzegovina*

[4] *University of Tuzla, Faculty of Mining Geology and Civil Engineering, Department of Civil Engineering, Univerzitetska, 2, 75000, Tuzla, Bosnia and Herzegovina*

Corresponding author:
Besim Demirović
besim_demirovic@yahoo.com

Received:
May 17, 2022

Accepted:
October 14, 2022

Published:
December 23, 2022

Citation:
Demirović, B.; Osmić, N.; Hadžović, R.; and Požegić, Z. (2022). Numerical Analysis of Geometric and Material Nonlinearity of Beams in the Plane. *Advances in Civil and Architectural Engineering*. Vol. 13, Issue No. 25. pp. 32-45
https://doi.org/10.13167/2022.25.4

ADVANCES IN CIVIL AND ARCHITECTURAL ENGINEERING (ISSN 2975-3848)

Faculty of Civil Engineering and Architecture Osijek
Josip Juraj Strossmayer University of Osijek
Vladimira Preloga 3
31000 Osijek
CROATIA

Abstract:
The paper presents a simultaneous numerical analysis of the geometric and material nonlinearity of the beams. It describes a process of determining the bearing capacity of a stratified cross-section of a beam made of homogeneous and isotropic material in linear and nonlinear domains of material behaviour. Material nonlinearity is analysed by the variation of the cross-sectional stiffness of the beam on bending EI in the stiffness matrix of the system obtained according to the first-order theory. Geometric nonlinearity is introduced into the calculation using the geometric stiffness matrix of the system. Numerical examples present an application of the procedure for solving problems of nonlinear structure analysis. The calculation results obtained in accordance with the procedure described in the paper are compared with the results of the SCIA software package.

Keywords:
numerical analysis; geometric nonlinearity; material nonlinearity

1 Introduction

The influence of geometric nonlinearity is introduced into the calculation of slender load-bearing elements under the influence of loads. An increase is noted in the cross-sectional forces, deformations, and displacements of the system that occur by changing the geometry of the system owing to the load. The equations describing the static and deformation states of a beam are divided into three groups: 1) equilibrium conditions, 2) compatibility conditions, and 3) constitutive equations [1]. Geometric nonlinearity encompasses the equilibrium conditions that are established in the deformed system and conditions of compatibility between the deformations of the cross section of the beam and the displacement of the axis of the beam. In most cases, in practice, the displacements of the system are small (finite displacement) but have sufficient intensity to establish balance conditions in the deformed system. The relationship between displacement and deformation are adopted as linear. Beam calculation, in which linear constitutive equations and compatibility conditions are adopted, and nonlinear conditions of balance are called the second-order theory.

In [2], spatial systems are analysed in accordance with the second-order theory. The stiffness matrix of the beam is obtained using the solution of the differential equation of the beam in accordance with the second-order theory. The results of the analysis are compared with those of the approximate solution of the geometric stiffness matrix. The approximate solution of the geometric stiffness matrix of the beam is based on the interpolation functions of the first-order theory of the beam. The results of the approximate calculation are close to the results of the calculation according to the second-order theory when the beams of the system are divided into smaller elements.

The constitutive equations describe the connections between the deformations and stress of the cross-section of the beam. In the linear theory of beam calculation, the dependence of the normal stress and longitudinal strain $\sigma = \sigma(\varepsilon)$, that is, shear stress and shear strain, $\tau = \tau(\gamma)$, are linear. Material nonlinearity is introduced into the calculation by adopting nonlinear connections between the deformations and stresses. The calculation of the beam, in which the nonlinearity of the material is analysed, is called the theory of plasticity. The theory of plasticity is divided into a 1) simplified theory and 2) strict theory. The calculation of girders according to the simplified theory of plasticity is based on the plastic behaviour of the material in the narrow zones of the system elements. The zones in which the material behaves plastically are known as plastic joints. Furthermore, the elastic behaviour of the material is applied to other parts of the system beams (EI = constant and EA = constant). The cross-sections of the beams must be able to rotate cross-section M-κ to achieve the moment of plasticity. The strict theory of plasticity encompasses the nonlinearity of the material along the elements of the system (EI ≠ constant and EA ≠ constant). The stiffness of the cross-section of beams EI and EA is determined based on the bearing capacity of the cross-section of the beam. This bearing capacity is determined based on the assumption that the cross-sections remain flat and are controlled by the support axis after deformation, and the influence of transverse forces on the bearing capacity is ignored. In the case of a reinforced concrete section, the concrete does not participate in the tensile strength; no slippage occurs between the concrete and the reinforcement, and the participation of the forks in the bending strength is neglected.

In [3], the stability of the framework is analysed using numerical calculation methods. Material nonlinearity is introduced by applying the tangent modulus of material elasticity. The change in the elastic modulus of the material affects the changes in the stiffness of the finite elements of the system. In the analysis of material nonlinearity, the stress behaviour of the material must be understood. In [4], the inelastic behaviour of steel when stretched to fracture is described. The behaviour of the material must be understood well to analyse material nonlinearity. The behaviour of the material under uniaxial stress is described by $\sigma - \varepsilon$ and $\tau - \gamma$ diagrams. The behaviour of the material for biaxial and triaxial stresses is described by the following models: the Tresca, von Mises, Mohr–Coulomb, and Drucker–Prager. The analysis of the system according to the strict theory of plasticity is performed using numerical methods.

Finite element methods are numerical methods that are applicable to nonlinear structural analysis. Methods for calculating geometric and material nonlinearity using the finite element method are described in [5]. The nonlinearity of a material is determined by the decrease in the stiffness of the cross-section of the finite element using numerical methods. The stiffness of the cross-section of the element for bending and axial stress is obtained from the elastic–plastic bearing capacity of the cross-sections of the nodes of the final element. In the case of simultaneous analysis of geometric and material nonlinearity, the interpolation function of the reduced stiffness of the cross-section of the beam is adopted to form the finite element stiffness matrix. The stiffness of the finite elements of the system is reduced to a limit at which the forces and displacements in the two iterative stages become approximately equal. The displacements and rotations of the nodes occur as unknown quantities in the nodes of the system. A nonlinear analysis of structures is convenient to perform using numerical calculation methods in which displacements and rotations of system nodes occur as unknowns. The unknown displacements and rotations of nodes are obtained from a system of algebraic nonlinear equations. The nonlinear equations are solved using iterative methods. The contribution to the iterative solution of algebraic nonlinear equations is presented in [6, 7].
With the development of computer programs, nonlinear analysis of supporters is performed according to the defined input data within the program. The shape and parameters of the material stress–deformation relation affect the behaviour of the supporter in the analysis of material and geometric nonlinearity. The input data in the programs are defined as numerical values, and then, the material behaviour model and numerical methods for solving the system of nonlinear equations are adopted in a given number of iterations. The supporter is discretised by one-dimensional (1D) finite elements using the proposed numerical procedure for geometrical and material nonlinearity analyses. Computer programs in nonlinear analysis discretise system elements using two-dimensional (2D) elements. The aim of the described numerical calculation is to present the flow of the calculation and results of the nonlinear analysis of the supporters when discretising the system with 1D elements. The results of the manual calculation of the displacement of the nodes of the 1D elements should be close to the numerical values of the displacement of the nodes of the 2D elements calculated by the SCIA program.

2 Beam Stiffness Matrix

The balance of the bearing system and the beam as its integral part under load is established at the deformed position of the system. The connections between the cross-sectional forces and the load and the connections between the displacement of the beam axis and the deformations of the cross-section of the beam are nonlinear. In most cases, introducing the assumption of small deformation values of the cross-section of the beam: ε <<1 and φ<<1 in the calculation of building structures is justified. In addition, squares and higher degrees of deformation values can be neglected. The three groups of equations that describe the static deformation state of the beam in the analysis of geometric nonlinearity are nonlinear equations of equilibrium conditions, linear constitutive equations, and compatibility conditions. The analysis of the beam with the described assumptions is called the second-order theory. In the analysis of structures, the second-order theory is important because the effects on compressed and stressed elements are obtained using the second-order theory. An inhomogeneous differential equation obtained from the equations describing the static deformation state of the beam, according to the second-order theory, can be expressed as follows [8]:

$$\frac{\mathrm{d}^2}{\mathrm{d}x^2}\left[EI(x)\frac{\mathrm{d}^2 v}{\mathrm{d}x^2}\right] - \frac{\mathrm{d}}{\mathrm{d}x}\left(H(x)\frac{\mathrm{d}v}{\mathrm{d}x}\right) = p_y - \frac{\mathrm{d}^2}{\mathrm{d}x^2}\left[EI(x)\cdot\alpha_t\frac{\Delta t}{h}\right] \tag{1}$$

In Equation (1), the unknown quantities are displacements *v* and components of the intersection forces H(x). Constant α_t represents the temperature coefficient of the material, and p_y denotes the transversal load of the beam. The increase in force H(x) is minimal in most

cases of system analysis. According to Equation (1), sufficient accuracy of the solution of the bending of the beam is achieved if H = S is considered, where S is the normal force in the beam determined by the first-order theory. The analysis of the beam in which the assumption H = S is accepted is called the linearised second-order theory. In the case of prismatic beams loaded with a transverse load p_y without temperature influence and with a constant bending stiffness EI = const. and axial force H = constant, the differential equation (1) can be expressed as follows:

$$\frac{\mathrm{d}^4 v}{\mathrm{d}x^4} \pm k^2 \frac{\mathrm{d}^2 v}{\mathrm{d}x^2} = \frac{p_y}{EI}; k^2 = \frac{S}{EI} \tag{2}$$

The interpolation functions required to determine the members of the beam stiffness matrix are obtained for p_y = 0, and the unit generalised displacements of the beam nodes are accepted.

2.1 Fixed-ends beam

The deformation line of a beam with rigid connections at the ends is a homogeneous solution of Equation (2) and can be expressed as follows [9]:

$$v(x) = \beta_1 + \beta_2 \cdot kx + \beta_3 \cdot \sin k\,x + \beta_4 \cdot \cos k\,x \tag{3}$$

where β_1, β_2, β_3, and β_4, are the unknown constants. According to Equation (3), the deformation line of the beam according to the second-order theory is a form of a trigonometric function. The calculation of the stiffness matrix of the beam can be simplified by adopting the deformation line of the beam in the form of the third-degree polynomial. The third-degree polynomial corresponds to a homogeneous solution of the differential equation for the bending of the beam in accordance with the first-order theory for rigid beam connections, as shown in Figure 1.

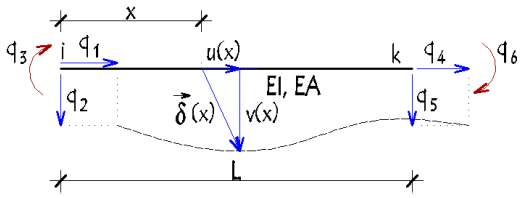

Figure 1. General line of displacement and deformation of a beam with fixed ends

The axial stress of the beam is described by an equation of the same form in the first- and second-order theories. The equations of axial stress and bending of the beam according to the first-order theory can be expressed as follows:

$$\frac{\mathrm{d}^2 u}{\mathrm{d}x^2} = 0; \frac{\mathrm{d}^4 v}{\mathrm{d}x^4} = 0 \tag{4}$$

The solution of the differential equation of the axial stress of the beam, considering the boundary conditions (x = 0 $\Rightarrow$ u = q_1, and x = L $\Rightarrow$ u = q_4), can be expressed as follows:

$$\begin{aligned} u(x) = \alpha_1 + \alpha_2 \cdot x = q_1 + \frac{q_4 - q_1}{L} x; u(x) = N_1(x) \cdot q_1 + N_4(x) \cdot q_4 \\ = \left(1 - \frac{x}{L}\right) \cdot q_1 + \frac{x}{L} \cdot q_4 \end{aligned} \tag{5}$$

where u(x) and v(x) denote the horizontal and vertical displacements, respectively, of the beam axis. The solution of the beam-bending equation can be expressed as follows:

$$v(x) = \alpha_1 + \alpha_2 \cdot x + \alpha_3 \cdot x^2 + \alpha_4 \cdot x^3; \frac{dv(x)}{dx} = \alpha_2 + 2\alpha_3 \cdot x + 3\alpha_4 \cdot x^2 \tag{6}$$

By introducing boundary conditions (x = 0 ⇒ v = q_2, dv/dx = q_3 i x = L ⇒ v = q_5, dv/dx = q_6) for the rigid connections of the beam, the deformation line can be expressed as follows:

$$v(x) = \left(1 - 3\frac{x^2}{L^2} + 2\frac{x^3}{L^3}\right)q_2 + \left(x - 2\frac{x^2}{L} + \frac{x^3}{L^2}\right)q_3 + \left(3\frac{x^2}{L^2} - 2\frac{x^3}{L^3}\right)q_5 + \left(\frac{x^3}{L^2} - \frac{x^2}{L}\right)q_6;$$
$$v(x) = \sum_i N_i q_i = N_2(x)\cdot q_2 + N_3(x)\cdot q_3 + N_5(x)\cdot q_5 + N_6(x)\cdot q_6 \quad (7)$$

Applying Castiglian theorem to the variation of the internal energy "U" of a beam, which occurs owing to the generalised displacement $q_i = 1$, generalised forces R_i can be obtained as follows [10]:

$$\frac{\partial U}{\partial \delta_i} = R_i \quad (8)$$

The internal energy of the beam from the generalised displacements of the beam nodes and axial pressure force determined by the first-order theory can be expressed as follows:

$$U = \frac{1}{2}\int_0^L \left[EA\left(\frac{\mathrm{d}u}{\mathrm{d}x}\right)^2 + EI\left(\frac{\mathrm{d}^2 v}{\mathrm{d}x^2}\right)^2 - S\left(\frac{\mathrm{d}v}{\mathrm{d}x}\right)^2\right]\mathrm{d}x \quad (9)$$

The first two terms of Equation (9) represent the energy from the axial stress and bending of the beam, respectively, and the third term represents the energy from the influence of the normal force when changing the geometry of the beam. After replacing the derivative of the beam axis displacement functions given by Equations (5), (7), and (9), the internal energy can be expressed as follows:

$$U = \frac{EA}{2L}(q_4^2 - 2q_4\cdot q_1 + q_1^2) + \frac{EI}{2}\left(\frac{12}{L^3}q_2^2 + \frac{4}{L}q_3^2 + \frac{12}{L^3}q_5^2 + \frac{4}{L}q_6^2 + \frac{12}{L^2}q_2\cdot q_3 - \frac{24}{L^3}q_2\cdot q_5 + \frac{12}{L^2}q_2\cdot q_6 - \right.$$
$$\left. - \frac{12}{L^2}q_3\cdot q_5 + \frac{4}{L}q_3\cdot q_6 - \frac{12}{L^2}q_5\cdot q_6\right) - \frac{S}{2}\left(\frac{6}{5L}q_2^2 + \frac{2L}{15}q_3^2 + \frac{6}{5L}q_5^2 + \frac{2L}{15}q_6^2 + \frac{1}{5}q_2\cdot q_3 - \right.$$
$$\left. - \frac{12}{5L}q_2\cdot q_5 + \frac{1}{5}q_2\cdot q_6 - \frac{1}{5}q_3\cdot q_5 - \frac{L}{15}q_3\cdot q_6 - \frac{1}{5}q_5\cdot q_6\right) \quad (10)$$

The terms of the stiffness matrix are defined as generalised forces arising from the accepted generalised displacements caused by single generalised displacements of the beam nodes. Generating internal potential energy on generalised displacements, the generalised forces in the matrix form of rigid connections of the beam are expressed as follows:

$$[R]^T = [R_1 \quad R_2 \quad R_3 \quad R_4 \quad R_5 \quad R_6] = \left[\frac{\partial U}{\partial q_1} \quad \frac{\partial U}{\partial q_2} \quad \frac{\partial U}{\partial q_3} \quad \frac{\partial U}{\partial q_4} \quad \frac{\partial U}{\partial q_5} \quad \frac{\partial U}{\partial q_6}\right] \quad (11)$$

$$[R] = \begin{bmatrix} \frac{EA}{L} & 0 & 0 & -\frac{EA}{L} & 0 & 0 \\ 0 & \frac{12EI}{L^3} - S\frac{6}{5L} & \frac{6EI}{L^2} - S\frac{1}{10} & 0 & -\frac{12EI}{L^3} + S\frac{6}{5L} & \frac{6EI}{L^2} - S\frac{1}{10} \\ 0 & \frac{6EI}{L^2} - S\frac{1}{10} & \frac{4EI}{L} - S\frac{2L}{15} & 0 & -\frac{6EI}{L^2} + S\frac{1}{10} & \frac{2EI}{L} + S\frac{L}{30} \\ -\frac{EA}{L} & 0 & 0 & \frac{EA}{L} & 0 & 0 \\ 0 & -\frac{12EI}{L^3} + S\frac{6}{5L} & -\frac{6EI}{L^2} + S\frac{1}{10} & 0 & \frac{12EI}{L^3} - S\frac{6}{5L} & -\frac{6EI}{L^2} + S\frac{1}{10} \\ 0 & \frac{6EI}{L^2} - S\frac{1}{10} & \frac{2EI}{L} + S\frac{L}{30} & 0 & -\frac{6EI}{L^2} + S\frac{1}{10} & \frac{4EI}{L} - S\frac{2L}{15} \end{bmatrix} \cdot \begin{bmatrix} q_1 \\ q_2 \\ q_3 \\ q_4 \\ q_5 \\ q_6 \end{bmatrix} \quad (12)$$

In general, Equation (12) can be written as follows:

$$[R] = [k] \cdot [q] = \left[[k_0] + \left[k_g\right]\right] \cdot [q] \tag{13}$$

where [R] denotes the vector of generalised forces, [k] denotes the stiffness matrix of the pressed beam that is represented as the sum of the stiffness matrix according to the first-order theory [k_0] and geometric matrix [k_g] obtained by an approximate solution, and [q] denotes the vector of the generalised displacements of the beam nodes.

2.2 One-sided fixed beam

By introducing the boundary conditions of a one-sided fixed beam into Equation (6) (x = 0 $\Rightarrow$ v = q_2, dv/dx = q_3 i x = L $\Rightarrow$ v = q_5), the deformation line can be written as follows:

$$\begin{aligned} v(x) &= \left(1 - \frac{3x^2}{2L^2} + \frac{x^3}{2L^3}\right) q_2 + \left(x - \frac{3x^2}{2L} + \frac{x^3}{2L^2}\right) q_3 + \left(\frac{3x^2}{2L^2} - \frac{x^3}{2L^3}\right) q_5 \\ &= N_2(x) \cdot q_2 + N_3(x) \cdot q_3 + N_5(x) \cdot q_5 \end{aligned} \tag{14}$$

A homogeneous solution of the differential equation of beam bending according to the theory of the first order of a one-sided fixed beam is a third-degree polynomial, as shown in Figure 2.

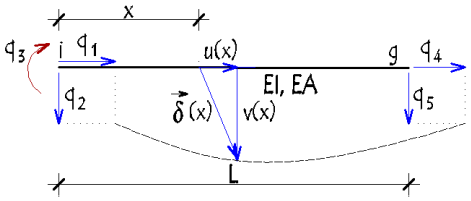

Figure 2. General line of displacement of a beam with fixed and hinged joints

The internal energy of a fixed beam based on Equations (5) and (14) can be expressed as follows:

$$\begin{aligned} U = \frac{EA}{2L}(q_4^2 - 2q_4 \cdot q_1 + q_1^2) + \frac{3EI}{2L^3}(q_2 + q_3 L - q_5)^2 \\ - \frac{S}{2}\left(\frac{2q_2 \cdot q_3}{5} - \frac{2q_3 \cdot q_5}{5} + \frac{6q_2^2}{5L} - \frac{12q_2 \cdot q_5}{5L} + \frac{6q_5^2}{5L} + \frac{q_3^2 L}{5}\right) \end{aligned} \tag{15}$$

Generalized forces in the matrix form of a one-sided fixed beam can be expressed as follows:

$$[R]^T = [R_1 \quad R_2 \quad R_3 \quad R_4 \quad R_5] = \left[\frac{\partial U}{\partial q_1} \quad \frac{\partial U}{\partial q_2} \quad \frac{\partial U}{\partial q_3} \quad \frac{\partial U}{\partial q_4} \quad \frac{\partial U}{\partial q_5}\right] \tag{16}$$

$$[R] = \begin{bmatrix} \frac{EA}{L} & 0 & 0 & -\frac{EA}{L} & 0 \\ 0 & \frac{3EI}{L^3} - S\frac{6}{5L} & \frac{3EI}{L^2} - S\frac{1}{5} & 0 & -\frac{3EI}{L^3} + S\frac{6}{5L} \\ 0 & \frac{3EI}{L^2} - S\frac{1}{5} & \frac{3EI}{L} - S\frac{L}{5} & 0 & -\frac{3EI}{L^2} + S\frac{1}{5} \\ -\frac{EA}{L} & 0 & 0 & \frac{EA}{L} & 0 \\ 0 & -\frac{3EI}{L^3} + S\frac{6}{5L} & -\frac{3EI}{L^2} + S\frac{1}{5} & 0 & \frac{3EI}{L^3} - S\frac{6}{5L} \end{bmatrix} \cdot \begin{bmatrix} q_1 \\ q_2 \\ q_3 \\ q_4 \\ q_5 \end{bmatrix} \tag{17}$$

In the case of a tension beam, the opposite signs are introduced before the elements in the geometric stiffness matrix. The solutions to the geometric nonlinearity problem are provided by an approximate procedure. The second-order influences are handled by an independent

geometric matrix of beam stiffness [k_g]. The nonlinearity of the material is introduced into the calculation of the stiffness matrix obtained according to the first-order theory.

3 Material Nonlinearity of the Beam

When analysing the material nonlinearity of a beam, the behaviour of the material under a load must be known. The behaviour of a material under axial stress is described by the normal stress–strain relationship. The stress–strain diagram of a material is approximated by adopted shapes such as bilinear, polygonal, and polynomial. Suitable forms of diagrams for the analysis of material nonlinearity are a) an ideal elastic–plastic diagram, b) an ideal elastic–plastic diagram with softening, and c) a nonlinear relation $\sigma - \varepsilon$, as shown in Figure 3.

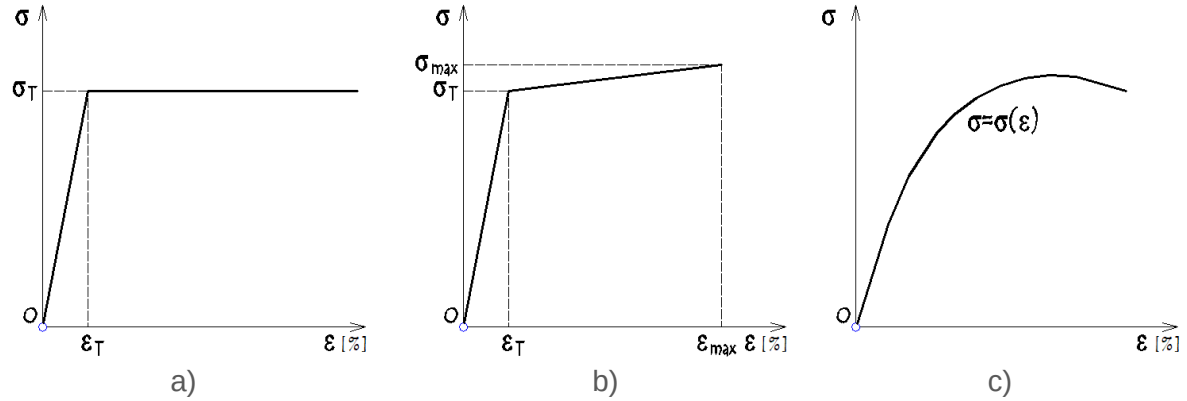

Figure 3. Behaviour of a material: a) ideal elastic–plastic diagram; b) elastic–plastic diagram with softening; c) nonlinear relation

In the following discussion, the diagram of elastic–plastic behaviour of the material with softening is analysed. Based on the accepted behaviour scheme of the material, the bearing capacity of the cross-section of the beam is determined. Modelling the load-bearing capacity of the cross-section of the beam is based on the following assumptions: the cross-section is symmetrical in relation to the vertical axis, cross-section forces act in the plane, and cross-sections remain straight and perpendicular to the beam axis before and after deformation. The load-bearing capacity of the cross-section of the beam is described by the ratios of the cross-sectional forces and deformations of cross-sections M-κ and N-ε. The secant modulus of elasticity of material E_s is valid up to the yield strength of material σ_T. After the yield strength of the material, the tangent modulus of the material, E_t, increases. The section is divided into equal layers of rib and flange, with thickness h_j, as shown in Figure 4. Each layer corresponds to deformation ε_j and normal stress σ_j. The stress of the individual layers in the elastic and plastic parts depends on deformation. Owing to the nonlinear behaviour of the material, this problem is solved iteratively [11].

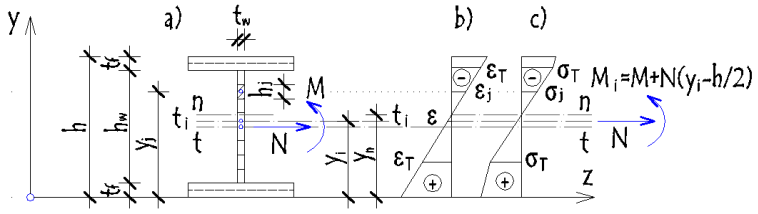

Figure 4. a) Layered cross-section; b) deformations of the cross-section; c) stresses of the cross-section

In the initial iterative step, the modulus of secant elasticity of the material, Es, is adopted for the selected combination of cross-sectional forces at the centroid of the cross-section. Based

on this, the deformation of the centroid cross-section of the section, curvature of the section, and deformation of the layers can be expressed as follows:

$$\varepsilon^{(0)} = \frac{N}{E_s A_i}; \kappa^{(0)} = \frac{M}{E_s I_i}; \varepsilon_j^{(0)} = \varepsilon + \kappa \cdot \left(y_i - y_j\right) \tag{18}$$

where $\varepsilon^{(0)}$ denotes the deformation of the centroid cross-section in the zero iterative step, and $\kappa^{(0)}$ denotes the curvature of the beam. The deformation of the *j*-th layer in the initial iteration corresponds to the deformation in the first iteration in accordance with the accepted stress diagram presented in Figure 4b.

$$\begin{aligned} &\sigma_j^{(1)} = E_s \cdot \varepsilon_j^{(0)} (0 \le \varepsilon \le \varepsilon_T); \\ &\sigma_j^{(1)} = \sigma_T + E_t \cdot \left(\varepsilon_j^{(0)} - \varepsilon_T\right) (\varepsilon_T \le \varepsilon \le \varepsilon_{max}()) \end{aligned} \tag{19}$$

where $\sigma_j^{(1)}$ denotes the stress of the j-th layer in the first iteration. If all the layers are in a state of elastic stress, the initial iterative step is sufficient. In the case of plastification of one or more layers, the iterative process continues until one of the cross-sectional layers cracks [12]. By integrating the stresses across the layers, intersection forces N i M of the first iteration are determined as follows:

$$N^{(1)} = \sum_j \sigma_j^{(1)} \cdot A_i ; M_i^{(1)} = \sum_j \sigma_j^{(1)} \cdot A_i \left(y_i - y_j\right) \tag{20}$$

In a new iterative step, the stiffness of the cross-section and position of the centroid cross-section are determined. For the *n*-th iteration, they can be expressed as follows:

$$\begin{aligned} &E^{(n)} A_i^{(n)} = \sum_j E_j^{(n)} \cdot A_j; E^{(n)} I_i^{(n)} = \sum_j E_j^{(n)} \cdot A_j \left(y_j - y_i\right)^2; \\ &\begin{bmatrix} (0 \le \varepsilon \le \varepsilon_T) \Rightarrow E_j^{(n)} = E_s \\ \left(\varepsilon_T \le \varepsilon \le \varepsilon_{max}()_j^{(n)}{}_t\right) \end{bmatrix}_i^{(n)} \frac{\sum_j E_j^{(n)} \cdot A_j \cdot y_j}{E^{(n)} A_i^{(n)}} \end{aligned} \tag{21}$$

The new characteristics of the cross-section correspond to the increment of deformations, curvature of the cross-section, increment of the normal force, and bending moment. They can be expressed as follows:

$$\Delta\varepsilon^{(n)} = \frac{\Delta N^{(n)}}{E^{(n)} A_i^{(n)}}; \Delta\kappa^{(n)} = \frac{\Delta M_i^{(n)}}{E^{(n)} I_i^{(n)}}; \Delta N^{(n)} = N - N^{(n-1)}; \Delta M_i^{(n)} = M_i - M_i^{(n-1)} \tag{22}$$

Deformations in the n-th iterative step and stresses of layer σ_j cross-sections in the n+1 step can be expressed as follows:

$$\begin{aligned} &\varepsilon^{(n)} = \varepsilon^{(n-1)} + \Delta\varepsilon^{(n)}; \kappa^{(n)} = \kappa^{(n-1)} + \Delta\kappa^{(n)}; \\ &\sigma_j^{(n+1)} = E_s \cdot \varepsilon_j^{(n)} (0 \le \varepsilon \le \varepsilon_T); \sigma_j^{(n+1)} = \sigma_T + E_t \cdot \left(\varepsilon_j^{(n)} - \varepsilon_T\right) (\varepsilon_T \le \varepsilon \le \varepsilon_{max}()) \end{aligned} \tag{23}$$

The iterative process is repeated until the increment in forces and deformations becomes small. The static and deformation characteristics of the beam change during the nonlinear analysis. The geometric characteristics of the cross-sections of the beam change with an increase in the load. Therefore, a numerical analysis of the static and deformation sizes of the beam can be performed at its discretisation points. By discretisation, the straight beam A-B is divided into finite elements of length L, as shown in Figure 5.

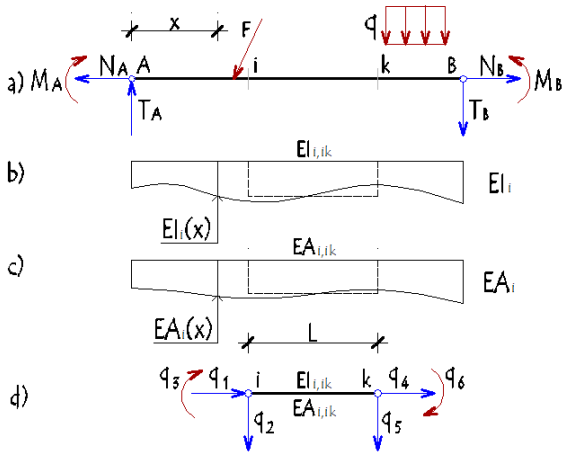

Figure 5. a) Beam A-B; b) change in stiffness EI_i of the beam; c) change in stiffness EA_i of the beam; d) finite element (short beam)

In the nodes of the finite elements, EA_i is the axial stiffness of the cross-section of the beam, and EI_i is the bending stiffness of the cross-section of the beam. When the final element is sufficiently small in length, the stiffness of the cross-section of beam i-k, $EA_{i,ik}$ and $EI_{i,ik}$, are assumed to have constant shape dimensions [13].

$$EA_{i,ik} = \frac{EA_{i,i} + EA_{i,k}}{2}; EI_{i,ik} = \frac{EI_{i,i} + EI_{i,k}}{2} \tag{24}$$

4 Beams Equilibrium Equations

After the introduction of the material nonlinearity of the finite element, the terms of the stiffness matrix according to the first-order theory have a variable value ($k_0 \neq$ const.). Geometric stiffness matrix $[k_g]$ is constant (k_g = const.) if the axial forces of the beam are accepted by the first-order theory. If the axial forces significantly change during the iterative process, matrix $[k_g]$ is corrected. The equilibrium equation of the system nodes in matrix form is expressed as follows [14]:

$$\left[\left[K_0^{(m-1)}\right] + \left[K_g\right]\right] \cdot \left[q^{(m)}\right] = [Q] + [S] \tag{25}$$

where $[K_0^{(m-1)}]$ denotes the stiffness matrix of the system according to the first-order theory in the (m-1) iterative step, $[K_g]$ denotes the geometric stiffness matrix of the system, $[q^{(m)}]$ denotes the matrix of displacement and rotation of nodes in the m-th iteration, [Q] denotes the vector of the equivalent nodal load, and [S] denotes the vector of the nodal forces. Matrix $[K_0^{(m-1)}]$ is defined as the material nonlinearity, and according to matrix $[k_g]$, the geometric nonlinearity of the system is defined. The system of Equation (25) is nonlinear; therefore, the solution of the system equations is determined iteratively. During the iterative process, the change in static and geometric quantities of $EI_{i,ik}$ and $EA_{i,ik}$ are handled by relations M-κ i N-ε . The iterative procedure continues until the *m*-th iteration when the stiffness of the system beams becomes approximately constant.

5 Numerical Examples

5.1 Example 1

In the numerical example in Figure 6, the bearing capacity of a simple beam is analysed under the action of the F and H forces. The load-bearing capacity of the beam is determined by the linear and nonlinear behaviours of the material, with and without the introduction of geometric nonlinearity. Input data: mechanical properties of steel material S 235 (σ_T = 235 MPa, σ_{max} =

360 MPa, $E_s = 2{,}1\times10^8$ kN/m^2). Figure 6b defines load capacity relation M- κ of cross-section b/h = 10/0,8 cm.

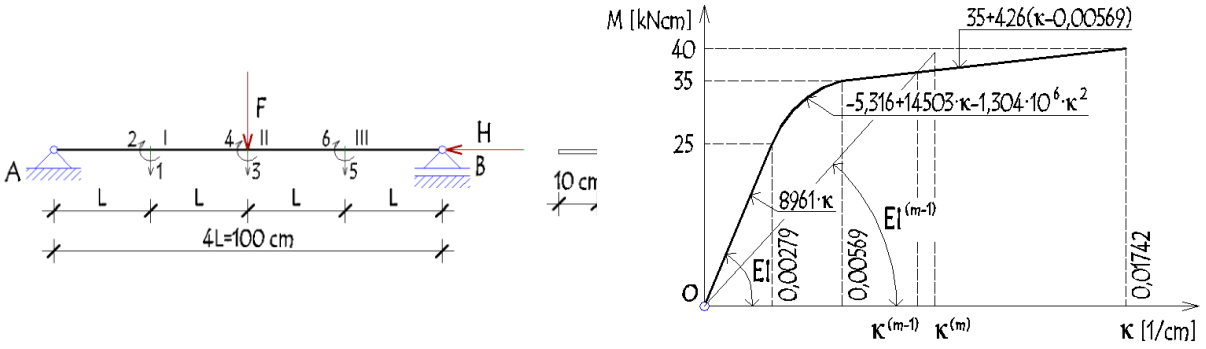

a) b)

Figure 6. Example 1: a) beam A-B; b) diagram of the bearing capacity of the cross section

The stiffness matrix of the system, equivalent nodal load vector, and displacement and rotation of the nodes are determined according to Figure 6. a) for the adopted generalised displacements as follows:

$$[K_0] = \begin{bmatrix} \frac{3EI_{A-I}}{L^3}+\frac{12EI_{I-II}}{L^3} & \frac{6EI_{I-II}}{L^2}-\frac{3EI_{A-I}}{L^2} & -\frac{12EI_{I-II}}{L^3} & \frac{6EI_{I-II}}{L^2} & 0 & 0 \\ \frac{6EI_{I-II}}{L^2}-\frac{3EI_{A-I}}{L^2} & \frac{3EI_{A-I}}{L}+\frac{4EI_{I-II}}{L} & -\frac{6EI_{I-II}}{L^2} & \frac{2EI_{I-II}}{L} & 0 & 0 \\ -\frac{12EI_{I-II}}{L^3} & -\frac{6EI_{I-II}}{L^2} & \frac{12EI_{I-II}}{L^3}+\frac{12EI_{II-III}}{L^3} & 0 & -\frac{12EI_{II-III}}{L^3} & \frac{6EI_{II-III}}{L^2} \\ \frac{6EI_{I-II}}{L^2} & \frac{2EI_{I-II}}{L} & 0 & \frac{4EI_{I-II}}{L}+\frac{4EI_{II-III}}{L} & -\frac{6EI_{II-III}}{L^2} & \frac{2EI_{II-III}}{L} \\ 0 & 0 & -\frac{12EI_{II-III}}{L^3} & -\frac{6EI_{II-III}}{L^2} & \frac{12EI_{II-III}}{L^3}+\frac{3EI_{III-B}}{L^3} & \frac{3EI_{III-B}}{L^2}-\frac{6EI_{II-III}}{L^2} \\ 0 & 0 & \frac{6EI_{II-III}}{L^2} & \frac{2EI_{II-III}}{L} & \frac{3EI_{III-B}}{L^2}-\frac{6EI_{II-III}}{L^2} & \frac{4EI_{II-III}}{L}+\frac{3EI_{III-B}}{L} \end{bmatrix} \quad (26)$$

$$[K_g] = H\cdot\begin{bmatrix} -\frac{12}{5L} & \frac{1}{10} & \frac{6}{5L} & -\frac{1}{10} & 0 & 0 \\ \frac{1}{10} & -\frac{L}{5}-\frac{2L}{15} & \frac{1}{10} & \frac{L}{30} & 0 & 0 \\ \frac{6}{5L} & \frac{1}{10} & -\frac{12}{5L} & 0 & \frac{6}{5L} & -\frac{1}{10} \\ -\frac{1}{10} & \frac{L}{30} & 0 & -\frac{4L}{15} & \frac{1}{10} & \frac{L}{30} \\ 0 & 0 & \frac{6}{5L} & \frac{1}{10} & -\frac{12}{5L} & -\frac{1}{10} \\ 0 & 0 & -\frac{1}{10} & \frac{L}{30} & -\frac{1}{10} & -\frac{L}{5}-\frac{2L}{15} \end{bmatrix}; [Q]+[S] = \begin{bmatrix} 0 \\ 0 \\ F \\ 0 \\ 0 \\ 0 \end{bmatrix}; [q] = \begin{bmatrix} v_1 \\ \phi_2 \\ v_3 \\ \phi_4 \\ v_5 \\ \phi_6 \end{bmatrix} \quad (27)$$

The solution of the matrix system of equations is iteratively performed incrementally. The deformation and forces in the selected increments are determined using the direct iteration method (the secant stiffness method). In the elastic area of the material behaviour, the increments of the F force are 0,5 kN. After the yield strength of the material is reached, the change in the increment of the F force is 0,1 kN. The results of the displacement ratio in the middle of beam v_3 and the F force in the linear analysis, analysis of geometric nonlinearity, and analysis of geometric and material nonlinearity are presented in Figure 7 and 8.

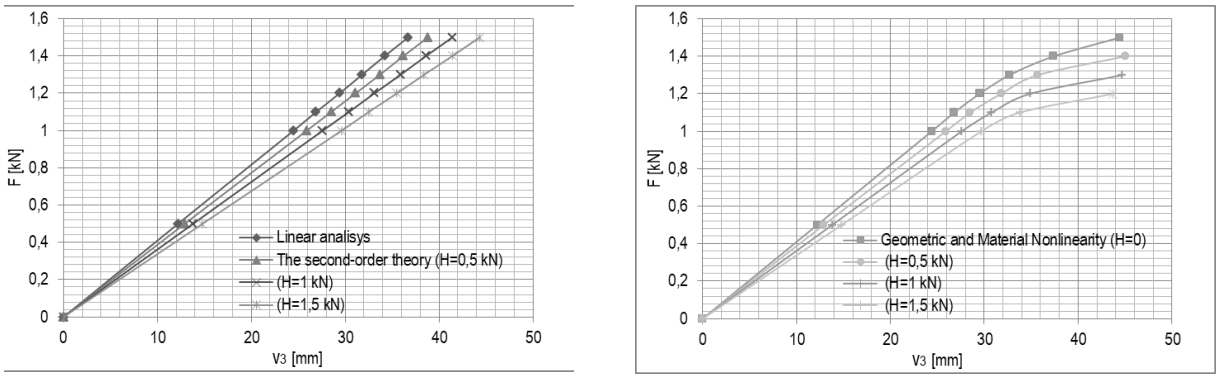

a) b)

Figure 7. Force–displacement relations: a) linear analysis and geometric nonlinearity analysis (EI = constant) [15]; b) analysis of geometric and material nonlinearity by the SCIA software package (EI ≠ constant) [15]

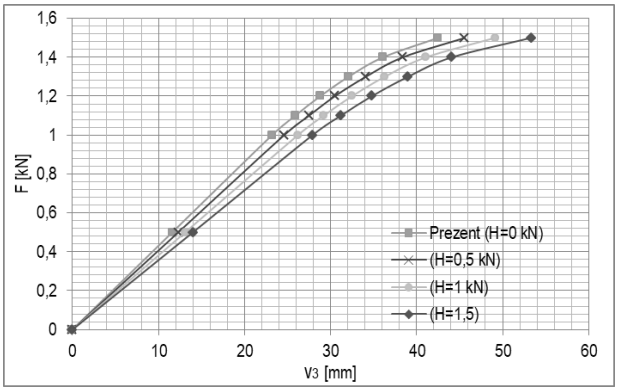

Figure 8. Force–displacement relations in the analysis of geometric and material nonlinearity according to the described procedure (EI ≠ constant)

The calculated results show a significant difference in the vertical displacement of the v_3 beam in the analysis of geometric nonlinearity and simultaneous analysis of geometric and material nonlinearity. In the analysis of geometric nonlinearity, a linear increase in the displacement is observed that is caused by a decrease in the stiffness of the system owing to changes in geometry. The displacement increment becomes nonlinear using the simultaneous analysis of geometric and material nonlinearity after reaching the material flow limit, as shown in Figure 8. When the normal force is higher, the yield strength of the cross-sectional material of the beam is reduced.

5.2 Example 2

In the numerical example shown in Figure 9. a), the displacements and rotations of the nodes of the finite elements of the frame are determined. The input data for the mechanical properties of the steel material are identical to those in Example 1. The frame girder is made of the HEA 120 profile, for which the M-k bearing capacity scheme is shown in Figure 9. b).

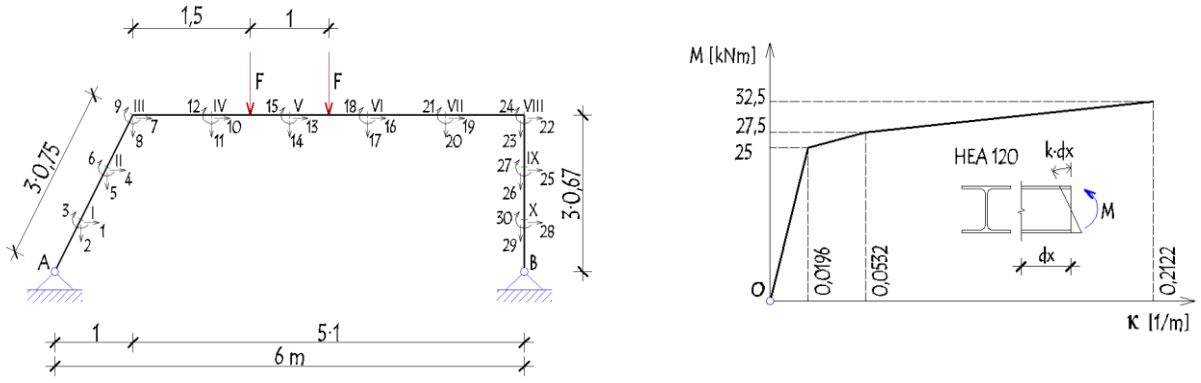

a) b)

Figure 9. Example 2: a) frame A-B; b) adopted relation of the bearing capacity of profile HEA 120

The load-bearing capacity of the beam is determined by the linear and nonlinear behaviours of the material, with and without the introduction of geometric nonlinearity.

Table 1. Results of horizontal displacement calculation q_{22} in node VIII

	Linear analysis	The Second Order Theory	Material nonlinearity	Geometric and material nonlinearity		Material nonlinearity	Difference (%)				
	I	II	III	IV	V	VI	$\frac{VI-III}{III}\cdot 100$	$\frac{V-IV}{IV}\cdot 100$	$\frac{VI-I}{I}\cdot 100$	$\frac{V-I}{I}\cdot 100$	$\frac{II-I}{I}\cdot 100$
2F (kN)	SCIA				Prezent						
	q22 (mm)						Δq22 (%)				
0	0,0	0,0	0,0	0,0	0,0	0,0	0,0	0,0	0,0	0,0	0,0
10	6,0	6,1	6,0	6,1	6,1	6,0	0,0	-0,6	0,0	1,1	1,7
20	12,0	12,3	12,0	12,3	12,3	12,0	0,0	0,0	0,0	2,5	2,5
30	18,0	18,7	18,1	18,8	18,7	17,9	-1,1	-0,6	-0,6	3,8	3,9
35	21,1	22,0	21,3	22,3	23,5	21,3	0,0	5,3	0,9	11,3	4,3
37,5	22,6	23,6	23,0	24,2	26,5	23,9	3,9	9,3	5,8	17,1	4,4
40	24,1	25,3	25,0	26,7	30,8	27,4	9,6	15,2	13,7	27,6	5,0
42,5	25,6	26,9	28,4	31,3	36,9	32,3	13,7	18,0	26,2	44,3	5,1
44	26,5	27,9	32,8	37,6	41,6	36,1	1,1	10,6	36,2	57,0	5,3
44,75	26,9	28,4	39,1	48,1	43,8	38,1	-2,6	-8,9	41,6	63,0	5,6

Figure 10. and Table 1. present an increase in the horizontal displacement in the 22 generalised directions, depending on load F. A comparison of the results of the proposed calculation and those of the calculation by the SCIA software package is presented in a comparative graphic presentation. In the elastic area of the material behaviour shown in Figure 10, the force–displacement relations are linear. After reaching the moment of the beginning of plastification of HEA 120 cross-section M_T = 25 kNm, until the moment of complete plastification of the cross-section, the force–displacement relations are nonlinear. The increase in system deformation is significant with a further increase in the load to the limit value. At the maximum load of the system, two cases can occur: 1) breakdown of one or more sections in which the system becomes a mechanism and 2) loss of stability of one or more elements of the system. In both cases, large (finite) displacements occur in the system.

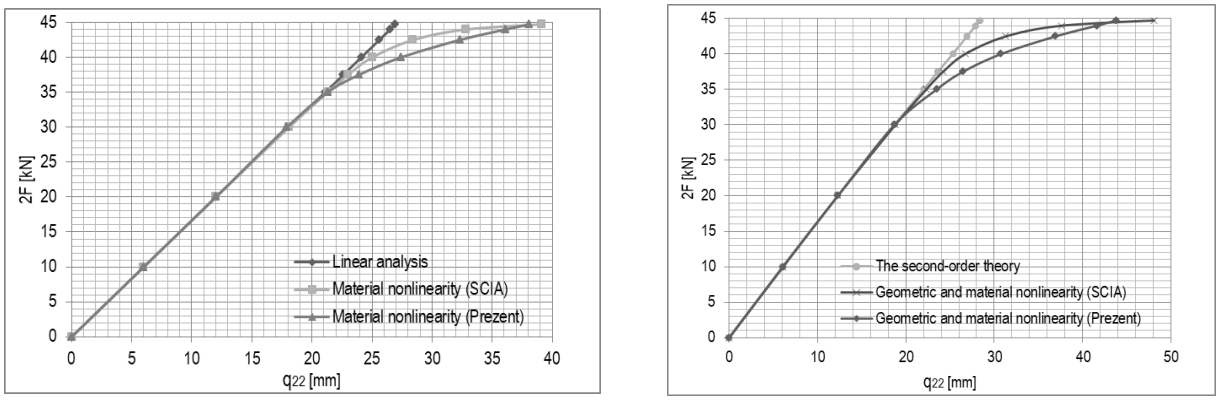

Figure 10. Force–displacement relations: a) analysis of material nonlinearity (EI ≠ constant); b) analysis of geometric and material nonlinearity (EI ≠ constant)

Node displacements and rotations are obtained from a system of nonlinear equations solved by iterative methods using the Mathematica software package [16].

6 Conclusions

The introduction of geometric nonlinearity in the calculation of load-bearing systems is justified in constructions with slender elements. Geometric nonlinearity is handled by the geometric stiffness matrix of a finite element (beam). The nonlinear behaviour of the material is analysed based on its nonlinearity. The study results conclude that the shifts in accordance with the second-order theory are 6% higher than those of the linear system analysis. The force–displacement ratio becomes nonlinear by introducing material nonlinearity into the calculation. In the case of the material behaviour above the yield strength, the displacements of the system calculated by introducing the nonlinearity of the material are 45% greater than the displacements in accordance with the linear theory. Using the simultaneous analysis of geometric and material nonlinearities, the displacements of the girders are approximately 63% greater than those according to the linear theory. The described calculation procedure provides solutions that describe the realistic behaviour of linear systems and determine the maximum load on the system. The load bearing on the girders is applied in increments ranging from zero to the maximum load.

The analysis of the numerical examples conclude that by increasing the slenderness of the elements of the system, the possibility of plasticising the material of the cross-section of the element decreases. In slender elements, a loss of stability occurs before the plastification of the material. The loss of stability is caused by a change in the geometry of the system owing to a decrease in the rigidity of the elements. The stiffness of the slender elements decreases with an increase in the normal forces.

Plastification of the material occurs when the elements are loaded during bending. Plastification first occurs at the node with the greatest bending moment. Plastification spreads to other zones of the elements; consequently, the rigidity of the entire system decreases with a further increase in the load. An increment in deformations and a redistribution of transverse forces occur with a decrease in the rigidity of the system.

The results of the described procedure are compared with those obtained by the SCIA software package, in which the system is modelled using 2D finite elements. The described procedure for analysing the geometric and material nonlinearity of the system is suitable for determining the ultimate load, bearing capacity of the system in the form of force displacement, and stability of individual elements of the system under the real behaviour of the system.

References

[1] Đurić, M. *Stabilnost i dinamika konstrukcija*. 1st Editon, Beograd, Serbia: Gradjevinski fakultet, 1980.

[2] Žugić, Lj.; Brčić, S.; Gopčević, Š. Programska realizacija proračuna prostornih linijskih nosača prema teoriji drugog reda. *Građevinar*, 2016, 68(5), pp. 381-398. https://doi.org/10.14256/JCE.1482.2015

[3] Brčić, S. Izvijanje okvirnih nosača u plastičnoj oblasti. *Zbornik radova Arhitektonsko-građevinskog fakulteta Niš*, 2010, 13. pp. 9-12.

[4] Dokšanović, T. et al. Stress–strain relationships and influence of testing parameters on coupon test results. *Advances in Civil and Architectural Engineering*, 2018, 9(16). pp. 50-63. https://doi.org/10.13167/2018.16.5

[5] Zienkiewicz, O. C.; Taylor, R. L. *The Finite Element Method*. 5th Edition, Oxford, UK: Butterworth-Heinemann, 2000.

[6] Rezaiee-Pajand, M.; Naserian, R. Nonlinear Frame Analysis by Minimization Technique. *International Journal of Optimization in Civil Engineering*, 2017, 7(2), pp. 291-318.

[7] Saffari, H. et al. Elasto-Plastic Analysis of Steel Plane Frames Using Homotopy Perturbation Method. *Journal of Constructional Steel Research*, 2012, 70. pp. 350-357. https://doi.org/10.1016/j.jcsr.2011.10.013

[8] Čaušević, M.; Bulić, M. *Stabilnost konstrukcija*. 1st Edition, Zagreb, Croatia: Golden marketing – Tehnička knjiga, 2013.

[9] Ranković, S. *Metode rešavanja zadataka stabilnosti*. 1st Edition, Beograd, Serbia: Gradjevinski fakultet, 1994.

[10] Hutton D. *Fundamentals of Finite Element Analysis*. 1st Edition, New York, USA: Mc Graw Hill, 2004.

[11] Demirović, B.; Osmić, N. Numerical analysis of reinforced concrete beam in two-dimensional form. *Advances in Civil and Architectural Engineering*, 2019, 10(18). pp. 36-47. https://doi.org/10.13167/2019.18.4

[12] Mihanović, A.; Marović, P.; Dvornik, J. *Nelinearni proračuni armirano betonskih konstrukcija*. 1st Edition, Zagreb, Croatia: Društvo hrvatskih građevinskih konstruktora, 1993.

[13] Maglajlić, Z. *Metoda relaksacije – Linearni i nelinearni problemi*. 1st Edition, Fojnica, BiH: Štamparija Fojnica, 2008.

[14] Sekulović, M. *Teorija linijskih nosača*. 1st Edition, Beograd, Seriba: Građevinska knjiga, 2005.

[15] SCIA Software. *Structural Analysis and Design Software*. Accessed: December 2022. Available at: https://www.scia.net/en

[16] Wolfram S. *Mathematical Book*. Champaign: Wolfram Media, 1998.